Available online at www.elixirpublishers.com (Elixir International Journal)

Applied Mathematics

Elixir Appl. Math. 60 (2013) 16373-16384

ISSN: 2229-712X

Radiation effects on a convective flow of a micropolar fluid along an inclined flat plate with uniform surface heat and mass flux

E. Manjoolatha, N. Bhaskar Reddy, T.Poornima and M.Prasanna Lakshmi
Department of Mathematics, Sri Venkateswara University, Tirupati – 517502.

ARTICLE INFO

Article history:
Received: 6 May 2013;
Received in revised form: 24 June 2013;
Accepted: 11 July 2013;

Keywords
Heat and Mass Transfer,
Radiation, MHD,
Micropolar fluid,
Heat generation/absorption.

ABSTRACT
A steady two dimensional free convective flow of an electrically conducting and radiating micropolar fluid along an inclined flat plate is investigated, by taking variable electrical conductivity, uniform surface heat flux and mass flux into account. The governing partial differential equations are transformed into a system of ordinary differential equations, which are then solved numerically by a fourth order Runge-Kutta method along with shooting technique. A parametric study is conducted to illustrate the effects of the governing parameters namely, micro-inertia density parameter, vertex viscosity parameter, heat generation/absorption parameter, radiation parameter, Schmidt number and Prandtl number on the velocity, temperature and concentration as well as skin-friction coefficient, Nusselt number and Sherwood number.

1. Introduction

Micropolar fluids are those, which contain micro-constituents that can undergo rotation, the presence of which can affect the hydrodynamics of the flow so that it can be distinctly non-Newtonian. These fluids are fluids with microstructure belonging to a class of complex fluids with nonsymmetrical stress tensor referred to as micromorphic fluids. It has many practical applications, for examples analyzing the behavior of exotic lubricants, the flow of colloidal suspensions or polymeric fluids, liquid crystals, additive suspensions, animal blood, body fluids, and turbulent shear flows. Ariman et al. [1] has given an excellent review of micropolar fluids and their applications. Hoyt and Fabula [2] have shown experimentally that the fluids containing minute polymeric additives indicate considerable reduction of the skin-friction (about 25-30%), a concept that can be well explained by the theory of micropolar fluids. Convective flow over a flat plate that is immersed in a micropolar fluid has attracted an increasing amount of attention since the early studies of Eringen [3].

Many transport processes occurring both in nature and in industries involve fluid flows with the combined heat and mass transfer. Such flows are driven by the multiple buoyancy effects arising from the density variations caused by the variations in temperature as well as species concentrations, for example, in atmospheric flows there exist differences in H_2O concentration and hence the flow is affected by such concentration difference. The first systematic study of mass transfer effects on free convection flow past a semi infinite vertical plate was presented by Gebhart and Pera [4] who presented a similarity solution to this problem and introduced a parameter N which is a measure of relative importance of chemical and thermal diffusion causing a density difference that drives the flow the parameter N is positive when both effects combined to drive the flow and it is negative when these effects are opposed. A mathematical model for the steady thermal convection heat and mass transfer in a micropolar fluid saturated Darcian porous medium in the presence of significant Dufour and Soret effects and viscous heating is presented by Rawat and Bhargava [5]. Joneidi et al [6] discussed the micropolar flow in a porous channel with high mass transfer

The study of magneto-hydrodynamic flow for electrically conducting fluid past heated surface has attracted the interest of many researches in view of its important applications in many engineering problems such as plasma studies, petroleum industries MHD power generations, cooling of nuclear reactors, the boundary layer control in aerodynamics and crystal growth. Until recently this study has been largely concerned with flow and heat transfer characteristics in various physical situations. Watanabe and Pop [7] investigated the heat transfer in the thermal boundary layer of magneto-hydrodynamic flow over a flat plate. Rahman and Sattar [8] analyzed the magnetohydrodynamic convective flow of a micropolar fluid past a continuously moving vertical porous plate in the presence of heat generation or absorption. Alam et al. [9] studied the effects of thermophoresis and chemical reaction on unsteady hydromagnetic free convection and mass transfer flow past an impulsively started infinite inclined porous plate in the presence of heat generation/absorption. Alam et al. [10] studied MHD free convective heat and mass transfer flow past an inclined surface with heat generation. Alam et al. [11] discussed the effects of variable suction and thermophoresis on steady MHD combined free-forced convective heat and mass transfer flow along a semi-infinite permeable inclined plat in the presence of thermal radiation. Molla et al. [12] investigated the natural convection flow along a heated wavy surface with a distributed heat source as given in Vajravelu and Hadjinolaou [13]. Mohammadein and Gorla [14] investigated heat transfer in a micropolar fluid over a stretching sheet with viscous dissipation and internal heat generation.

Heat transfer by simultaneous radiation and convection has applications in numerous technological problems, including combustion, furnace design, the design of high temperature gas cooled nuclear reactors, nuclear reactor safety, fluidized bed heat exchanger, fire spreads, advance energy conversion devices such as open cycle coal and natural gas fired MHD, solar fans, solar

Tele:
E-mail addresses: elavarthimanjoo@gmail.com

collectors natural convection in cavities, turbid water bodies, photo chemical reactors and many others when heat transfer by radiation is of the same order of magnitude as by convection, a separate calculation of radiation and convection and their superposition without considering the interaction between them can lead to significant errors in the results, because of the presence of the radiation in the medium, which alters the temperature distribution within the fluid. Therefore, in such situation heat transfer by convection and radiation should be solved for simultaneously. In this context, Ishak [15] studied the thermal boundary layer flow induced by a linearly stretching sheet immersed in an incompressible micropolar fluid with constant surface temperature and found that the heat transfer rate at the surface decreases in the presence of radiation. Muhammad Ashraf and Muhammad Rashid [16] discussed the MHD boundary layer stagnation point flow and heat transfer of a micropolar fluid towards a heated shrinking sheet with radiation and heat generation. Ahmed Yousof Bakier [17] has analyzed the natural convection heat and mass transfer in a micropolar fluid- saturated non-Darcy porous regime with radiation and thermophoresis effects. Rahman and Sattar [18] studied transient convective flow of micropolar fluid past a continuously moving vertical porous plate in the presence of radiation.

Mansour et al. [19] studied heat and mass transfer effects on magnetohydrodynamic flow of a micropolar fluid on a circular cylinder with uniform heat and mass flux. Damseh et al [20] discussed an unsteady natural convection heat transfer of micropolar fluid over a vertical surface with constant heat flux. Srinivasacharya and Ramreddy [21] analyze the effects of Soret and Dufour on mixed convection heat and mass transfer in a micropolar fluid with heat and mass fluxes. Jashim Uddin [22] has discussed the convective flow of micropolar fluids along an inclined flat plate with variable electric conductivity and uniform surface heat flux. Rahman and Sultana [23] studied radiative heat transfer flow of micropolar fluid past a vertical porous flat plate with uniform plate temperature as well as variable surface heat flux in a porous medium. Markin and Mahmood [24] obtained similarity solutions for the mixed convection flow over a vertical plate for the case of constant heat flux condition at the wall.

The aim of the present study is to analyze a steady MHD free convective flow of an incompressible electrically conducting and radiating micropolar fluid along an inclined flat plate with uniform surface heat flux and uniform surface mass flux. The governing boundary layer equations have been transformed to a two-point boundary value problem in similarity variables and the resultant problem is solved numerically using the Runge-Kutta method with shooting technique. The effects of various governing parameters on the fluid velocity, temperature, concentration, skin-friction coefficient, Nusselt number and Sherwood number are shown in figures and tables and discussed in detail.

2. Mathematical Formulation

A steady two-dimensional laminar free convective flow of an incompressible, electrically conducting and radiating micropolar fluid along a semi-infinite inclined flat plate with an acute angle α to the vertical, is considered. The *x* - axis is taken along the inclined plate and *y*-axis normal to it. A uniform magnetic field of strength *B(x)* is assumed to be in the *y* - direction. The magnetic Reynolds number is taken to be small enough so that the induced magnetic field, Hall effects and Joule heating are negligible. The level of concentration of foreign mass is assumed to be low, so that the Soret and Dufour effects are negligible. Under these assumptions along with the Boussinesq's and boundary layer approximations, the system of equations which governs the flow field are

$$\frac{\partial u}{\partial x}+\frac{\partial v}{\partial y}=0 \tag{1}$$

$$u\frac{\partial u}{\partial x}+v\frac{\partial u}{\partial y}=\left(\upsilon+\frac{S}{\rho}\right)\frac{\partial^2 u}{\partial y^2}+\frac{S}{\rho}\frac{\partial \sigma}{\partial y}-\frac{\sigma_0^{'}(B(x))^2 u}{\rho}+g\beta_T(T-T_\infty)Cos\alpha+g\beta_C(C-C_\infty)Cos\alpha \tag{2}$$

$$\rho j\left(u\frac{\partial \sigma}{\partial x}+v\frac{\partial \sigma}{\partial y}\right)=\upsilon_s\frac{\partial^2 \sigma}{\partial y^2}-S\left(2\sigma+\frac{\partial u}{\partial y}\right) \tag{3}$$

$$u\frac{\partial T}{\partial x}+v\frac{\partial T}{\partial y}=\frac{k}{\rho c_p}\frac{\partial^2 T}{\partial y^2}-\frac{1}{\rho c_p}\frac{\partial q_r}{\partial y}+\frac{Q_0}{\rho c_p}(T-T_\infty) \tag{4}$$

$$u\frac{\partial C}{\partial x}+v\frac{\partial C}{\partial y}=D\frac{\partial^2 C}{\partial y^2} \tag{5}$$

The boundary conditions for the velocity, temperature and concentration fields are

$$u=0, v=0, \sigma=-n\frac{\partial u}{\partial y}, \frac{\partial T}{\partial y}=-\frac{q_w}{k}, \frac{\partial C}{\partial y}=-\frac{M_n}{D} \quad \text{at} \quad y=0$$
$$u\to 0, \sigma\to 0, T\to T_\infty, C\to C_\infty \quad \text{as} \quad y\to\infty \tag{6}$$

where u, v are the velocity components along x, y co-ordinates respectively, υ is the kinematic viscosity, ρ is the mass density of the fluid, μ is the coefficient of dynamic viscosity, υ_s is the microrotation viscosity or spin-gradient viscosity, S is the microrotation coupling coefficient (also known as the coefficient of gyro-viscosity or as the vortex viscosity), q_w is the surface heat flux, M_n is the surface mass flux, σ is the microrotation component normal to the xy - plane, j is the micro-inertia density, T is the temperature of the fluid in the boundary layer and C is the fluid concentration in the boundary layer, T_∞ is the temperature of the fluid outside the boundary layer, c_p is the specific heat of the fluid at constant pressure, k is the thermal conductivity, g is the acceleration due to gravity, β_T is the thermal expansion coefficient, β_C is the coefficient of expansion with concentration, q_r is the radiative heat flux and D is the coefficient of mass diffusivity.

In the present work we assume that the micro-inertia density j is constant. For the flow under study, it is relevant to assume that the applied magnetic field strength $B(x)$ has the form

$$B(x) = \frac{B_0}{\sqrt{x}} \tag{7}$$

where B_0 is a constant. Moreover, the electrical conductivity $\sigma_0^{'}$ is assumed to have the form

$$\sigma_0^{'} = \sigma_0 u \text{, where } \sigma_0 \text{ is a constant.} \tag{8}$$

In view of (7) and (8), the term $\dfrac{\sigma_0^{'}(B(x))^2 u}{\rho}$ can be written as

$$\frac{\sigma_0^{'}(B(x))^2 u}{\rho} = \frac{\sigma_0 B_0^2 u^2}{\rho x} \tag{9}$$

Using (9), the momentum equation (2) can be written as

$$u\frac{\partial u}{\partial x} + v\frac{\partial u}{\partial y} = \left(\upsilon + \frac{S}{\rho}\right)\frac{\partial^2 u}{\partial y^2} + \frac{S}{\rho}\frac{\partial \sigma}{\partial y} - \frac{\sigma_0 B_0^2 u^2}{\rho x} + g\beta_T (T - T_\infty)Cos\alpha + g\beta_C (C - C_\infty)Cos\alpha \tag{10}$$

By using the Rosseland approximation (Brewster [25]), the radiative heat flux q_r is given by

$$q_r = -\frac{4\sigma *}{3K'}\frac{\partial T^4}{\partial y} \tag{11}$$

where $\sigma *$ is the Stefan-Boltzmann constant and K' - the mean absorption coefficient. It should be noted that by using the Rosseland approximation, the present analysis is limited to optically thick fluids. If temperature differences within the flow are sufficiently small, then Equation (11) can be linearized by expanding T^4 into the Taylor series about T_∞, which after neglecting higher order terms takes the form

$$T^4 \cong 4T_\infty^3 T - 3T_\infty^4 \tag{12}$$

In view of the equations (11) and (12), the equation (4) reduces to

$$u\frac{\partial T}{\partial x} + v\frac{\partial T}{\partial y} = \alpha\left(1 + \frac{16\sigma * T_\infty^3}{3K'k}\right)\frac{\partial^2 T}{\partial y^2} + \frac{Q_0}{\rho c_p}(T - T_\infty) \tag{13}$$

The continuity equation (1) is satisfied by the Cauchy Riemann equations

$$u = \frac{\partial \psi}{\partial y} \quad \text{and} \quad v = -\frac{\partial \psi}{\partial x} \tag{14}$$

where $\psi(x, y)$ is the stream function.

In order to transform equations (10), (13) and (5) into a set of ordinary differential equations, the following similarity transformations and dimensionless variables are introduced.

$$f(\eta) = \frac{\psi}{(2\upsilon U_0 x)^{1/2}}, \quad \eta = y\sqrt{\frac{U_0}{2\upsilon x}}, \quad \sigma = \sqrt{\frac{U_0^3}{2\upsilon x}}h(\eta), \quad \upsilon_s = (\mu + \frac{S}{2})j,$$

$$T - T_\infty = \theta(\eta)T^*, \; C - C_\infty = \phi(\eta)C^*, \; T^* = \sqrt{\frac{2\upsilon x}{U_0}}\left(\frac{q_w}{k}\right), \; C^* = \sqrt{\frac{2\upsilon x}{U_0}}\left(\frac{M_n}{D}\right), \; M = \frac{2\sigma_0 B_0^2}{\rho}, \; \Delta = \frac{S}{\mu}, \; Gr = \frac{2g\beta_T T^* x}{U_0^2},$$

$$Gc = \frac{2g\beta_C C^* x}{U_0^2}, \quad \xi = \frac{jU_0}{\upsilon x}, \quad \Pr = \frac{\upsilon}{\alpha}, \quad Sc = \frac{\upsilon}{D}. \quad R = \frac{K'k}{4\sigma^* T_\infty^3}, \quad Q = \frac{2Q_0 x}{\rho c_p U_0} \tag{15}$$

where U_0 is some reference velocity, $f(\eta)$ - the dimensionless stream function, θ - the dimensionless temperature, ϕ - the dimensionless concentration, η - the similarity variable, M - the magnetic parameter, Gr - the local thermal Grashof number, Gc - the local solutal Grashof number, ξ - the micro-inertia density parameter, Δ - the vertex viscosity parameter, Pr - the Prandtl number, Sc - the Schmidt number, R - the radiation parameter and Q - the heat generation/absorption parameter.

In view of the equations (14) and (15), the equations (10), (13) and (5) transform into

$$(1+\Delta) f''' + ff'' + \Delta h' - Mf'^2 + Gr\theta Cos\alpha + Gc\phi Cos\alpha = 0 \tag{16}$$

$$(1+\Delta/2)\xi h'' + \xi(fh' + f'h) - 2\Delta(2h + f'') = 0 \tag{17}$$

$$\left(1+\frac{4}{3R}\right)\theta'' + \Pr(f\theta' - f'\theta) + \Pr Q\theta = 0 \tag{18}$$

$$\phi'' + Scf\phi' - Scf'\phi = 0 \tag{19}$$

The corresponding boundary conditions are

$$f=0,\ f'=0, h=-nf'', \theta'=-1, \phi'=-1 \quad \text{at} \quad \eta=0$$
$$f'=0, h=\theta=\phi=0. \quad \text{as} \quad \eta\to\infty \tag{20}$$

where the primes denote differentiation with respect to η

The physical quantities of interest are the skin friction coefficient C_f, plate couple stress M_x, the local Nusselt number Nu_x and Sherwood number Sh_x.

The skin-friction co-efficient is defined by

$$C_f = (2\,\mathrm{Re}_x^{-1})^{\frac{1}{2}}[1+(1-n)\Delta] f''(0) \tag{21}$$

Thus from equation (21), we see that the local values of the skin-friction C_f is proportional to $f''(0)$.

The dimensionless couple stress is defined by

$$M_x = (1+\frac{1}{2}\Delta)\xi h'(0) \tag{22}$$

Thus the local plate couple stress at the boundary layer is proportional to $h'(0)$.

The rate of heat transfer, in terms of the dimensionless Nusselt number is given by

$$Nu_x = (2^{-1}\,\mathrm{Re}_x)^{1/2}\frac{1}{\theta(0)} \tag{23}$$

Thus from equation (23), we see that the local Nusselt number Nu_x is proportional to $1/\theta(0)$

The rate of mass transfer, in terms of the dimensionless Sherwood number is given by

$$Sh_x = (2^{-1}\,\mathrm{Re}_x)^{1/2}\frac{1}{\phi(0)} \tag{24}$$

Thus from equation (24), we see that the local Sherwood number Sh_x is proportional to $1/\phi(0)$.

3. SOLUTION OF THE PROBLEM

The set of coupled non-linear governing boundary layer equations (16) - (19) together with the boundary conditions (20) are solved numerically by using Runge-Kutta fourth order technique along with shooting method. First of all, higher order non-linear differential Equations (16) - (19) are converted into simultaneous linear differential equations of first order and they are further transformed into initial value problem by applying the shooting technique (Jain *et al*.[26]). The resultant initial value problem is solved by employing Runge-Kutta fourth order technique. The step size $\Delta\eta$ =0.05 is used to obtain the numerical solution with five decimal place accuracy as the criterion of convergence. From the process of numerical computation, the skin-friction coefficient, the Nusselt number and the

Sherwood number, which are respectively proportional to $f''(0), 1/\theta(0)$ and $1/\phi(0)$, are also sorted out and their numerical values are presented in a tabular form.

4. Results And Discussion

In order to get a clear insight of the physical problem, the velocity, temperature and concentration have been discussed by assigning numerical values to the parameters encountered in the problem. The effects of various parameters on the velocity in the boundary layer are depicted in Figs. 1-7. The effects of various parameters on the microrotation in the boundary layer are depicted in Figs.8-12. The effects of various parameters on the temperature in the boundary layer are depicted in Figs. 13-18. The effects of various parameters on the concentration in the boundary layer are depicted in Figs. 19-23.

Fig. 1 shows the dimensionless velocity profiles for different values of magnetic parameter (*M*). It is seen that, as expected, the velocity decreases with an increase of magnetic parameter. The magnetic parameter is found to retard the velocity at all points of the flow field. It is because that the application of transverse magnetic field will result in a resistive type force (Lorentz force) similar to drag force which tends to resist the fluid flow and thus reducing its velocity. Also, the boundary layer thickness decreases with an increase in the magnetic parameter. Fig.2 illustrates the effect of the thermal Grashof number (*Gr*) on the velocity field. The flow is accelerated due to the enhancement in buoyancy force corresponding to an increase in the thermal Grashof number, i.e. free convection effects. It is noticed that the thermal Grashof number influence the velocity field almost in the boundary layer when compared to far away from the plate. It is seen that as the thermal Grashof number increases, the velocity field increases. The effect of solutal Grashof number (*Gc*) on the velocity is illustrated in Fig.3. It is noticed that the velocity increases with increasing values of the solutal Grashof number. Fig.4 illustrates the effect of vortex viscosity parameter (Δ) on the velocity. It is noticed that as the vortex viscosity parameter increases, the velocity decreases. The effect of the angle of inclination (*α*) on the velocity field is shown in Fig.5. From this figure we see that velocity decreases with the increase of α. As α increase the effect of the buoyancy force decreases since it is multiplied by Cos *α,* so the velocity profile decreases. Fig. 6 shows the variation of the velocity with the radiation parameter (*R*). It is noticed that the velocity increases with an increase in the radiation parameter. Fig. 7 depicts the velocity with the heat generation/absorption parameter (*Q*). It is noticed that the velocity increases with an increase in the heat generation/absorption parameter. The effect of the magnetic parameter (*M*) on the angular velocity is illustrated in Fig.8. It is observed that as the magnetic parameter increases, near the plate the microrotation increases and for away plate the microrotation decreases. Fig.9 shows the effect of vortex viscosity parameter Δ on the microrotation. It is seen that as the vortex viscosity parameter increases the microrotation increases near the plate and the trend gets reversed away from the plate. Fig.10 shows the effect of angle of inclination α in the microrotation. It is observe that as α increase, the microrotation increases near the plate and it decreases away from the plate. From Fig.11 It is seen that the microrotation decreases very rapidly with the increase of the micro-inertia density parameter. The effect of the radiation parameter (*R*) on the velocity is illustrated in Fig.12. It is observed that as the radiation parameter increases, near the plate the angular velocity decreases and for away plate the angular velocity increases.

The effect of the magnetic parameter (*M*) on the temperature is illustrated in Fig.13. It is observed that as the magnetic parameter increases, the temperature decreases. The effect of the vortex viscosity parameter on the temperature is illustrated in Fig.14. It is seen that as the vortex viscosity parameter increases, the temperature decreases. Fig. 15 depicts the temperature with the angle of inclination parameter (*α*). It is noticed that the temperature decreases with an increase in the angle of inclination parameter. Fig. 16 depicts the temperature with the Prandtl number (*Pr*). It is noticed that the temperature increases with an increase in the Prandtl number.

Fig.17 illustrates the effect of the radiation parameter (*R*) on the temperature. It is noticed that as the radiation parameter increases, the temperature increases. Fig. 18 shows the variation of the temperature with the heat generation/absorption parameter (*Q*). It is observed that the temperature increases with an increase in the heat generation/absorption parameter.

The effect of magnetic parameter (*M*) on the concentration field is illustrated Fig.19 As the magnetic parameter increases the concentration is found to be decreasing. The effect of vertex viscosity parameter on the concentration field is illustrated Fig. 20. It is noticed that the concentration decreases with an increase in the vertex viscosity parameter. The effect of angle of inclination parameter on the concentration field is illustrated Fig. 21. It is noticed that the concentration decreases with an increase in the angle of inclination parameter. Fig. 22 illustrates the effect of Schmidt number (*Sc*) on the concentration. As the Schmidt increases, an increasing trend in the concentration field is noticed. The influence of the heat generation/absorption parameter (*Q*) on the concentration field is shown in Fig.23. It is noticed that the concentration increases monotonically with the increase of the heat generation/absorption parameter.

In Figs.24-27, respectively, we represent the physical parameters skin-friction coefficient, plate couple stress, Nusselt number and Sherwood number for different values of *R* and vertex viscosity parameter Δ From Fig. 24, it is seen that skin-friction decreases rapidly with the increase of Δ and it increases with the increase of radiation parameter. From Fig. 25 it is observed that the plate couple stress increases rapidly with the increase of Δ as well as *R*. Again from the Fig. 26, it is noticed that Nusselt number increases rapidly with the increase of Δ and it decreases with the increase of radiation parameter. From Fig. 27, it is found that the Sherwood number increases with increase of Δ and it decreases with the increase of radiation parameter.

Figs.28-31, respectively, shows that skin-friction coefficient, plate couple stress, Nusselt number and Sherwood number for different values of magnetic parameter (*M*) and microrotation parameter (*n*). From Fig. 28, it is seen that skin-friction decreases rapidly with the increase of microrotation parameter (*n*) and it decreases with the increase of magnetic parameter. From Fig. 29, it is observed that the plate couple stress increases rapidly with the increase of microrotation parameter (*n*) and it decreases with the increase of magnetic parameter. Again from the Fig. 30, it is noticed that Nusselt number decreases rapidly with the increase of *n* and it increases with the increase of *M*. From Fig.31, it is found that the Sherwood number decreases with increase in *n* and it increases with the increase of *M*.

5 Conclusions

In the present problem, a steady MHD convective flow of an incompressible, electrically conducting and radiating micropolar fluid flow along an inclined flat plate with uniform surface heat flux and uniform surface mass flux is analyzed. Numerical calculations are carried out for various values of the dimensionless parameters of the problem. From the present calculation we may conclude that skin-friction coefficient (viscous drag) decreases monotonically with the increase of magnetic parameter, vortex viscosity parameter, angle of inclination. This coefficient increases with the increase of radiation parameter. Plate couple stress increases with the increase of radiation parameter or magnetic parameter or microrotation parameter while it decreases with the increase of the magnetic parameter. The heat transfer rate increases with the increase of magnetic parameter, vortex viscosity parameter. This rate of heat transfer is forced to decrease radiation parameter or microrotation parameter. The mass transfer rate increases with the increase of magnetic parameter or vortex viscosity parameter. This rate of mass transfer is forced to decrease with the increase of radiation parameter or microrotation parameter.

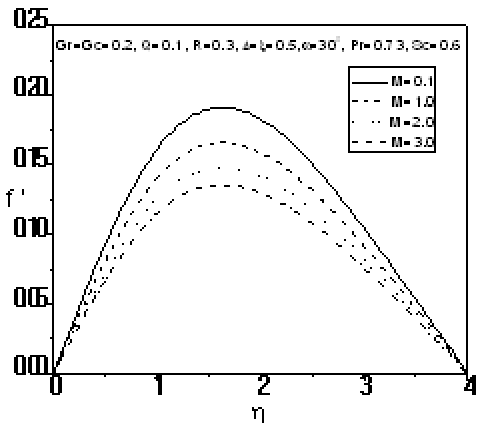

Fig.1 Velocity profiles for different values of *M*

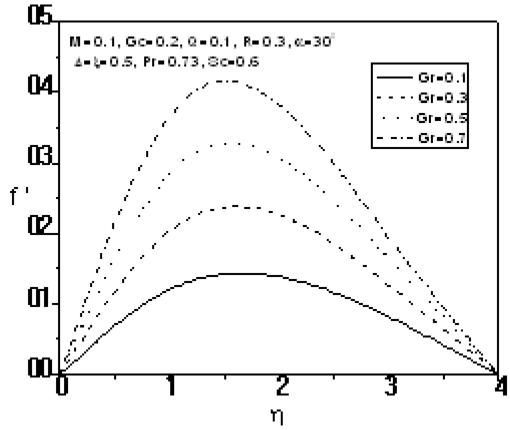

Fig.2 Velocity profiles for different values of *Gr*

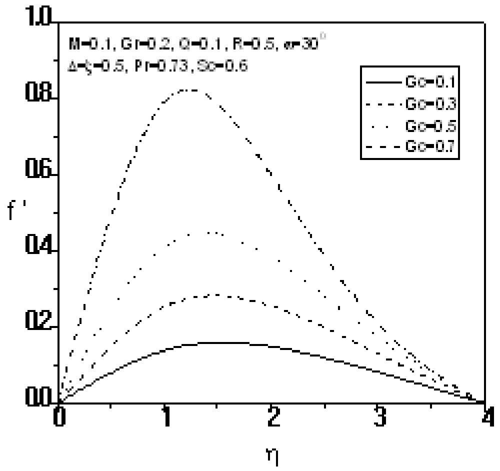

Fig.3 Velocity profiles for different values of *Gc*

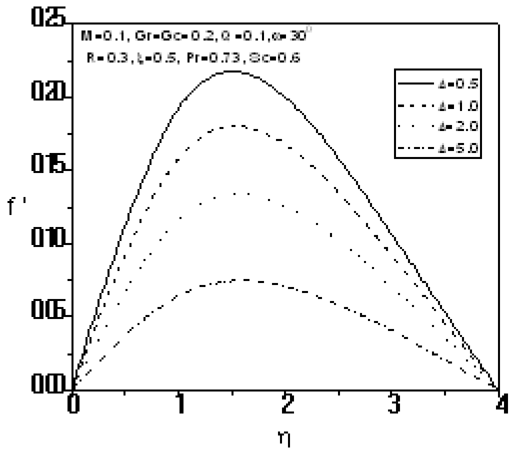

Fig.4 Velocity profiles for different values of Δ

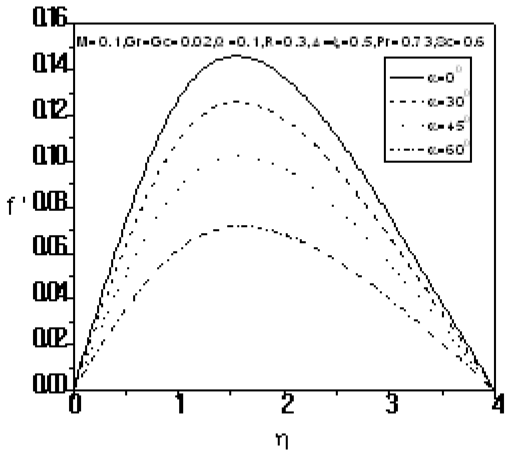

Fig.5 Velocity profiles for different values of *α*

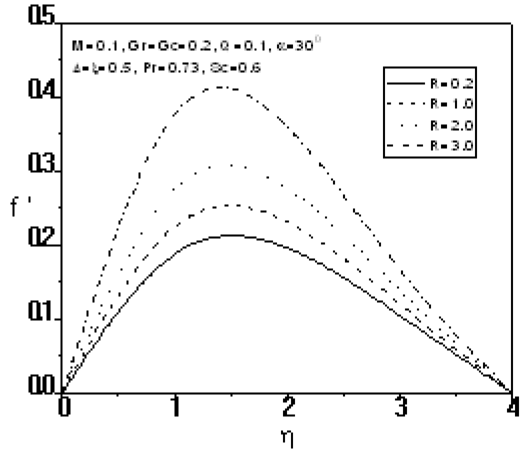

Fig.6 Velocity profiles for different values of *R*

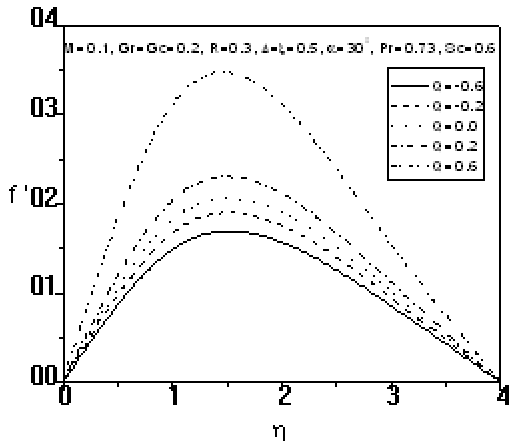

Fig.7 Velocity profiles for different values of *Q*

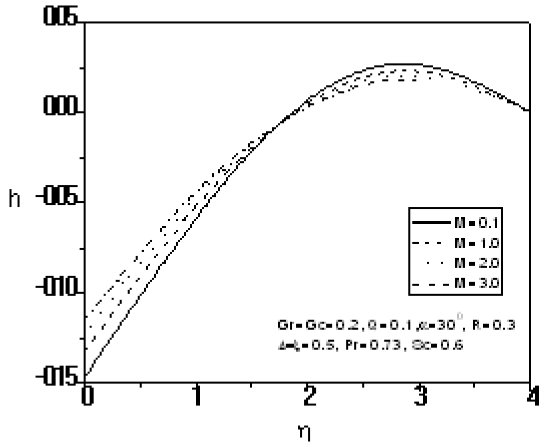

Fig.8 Angular velocity profiles for various *M*

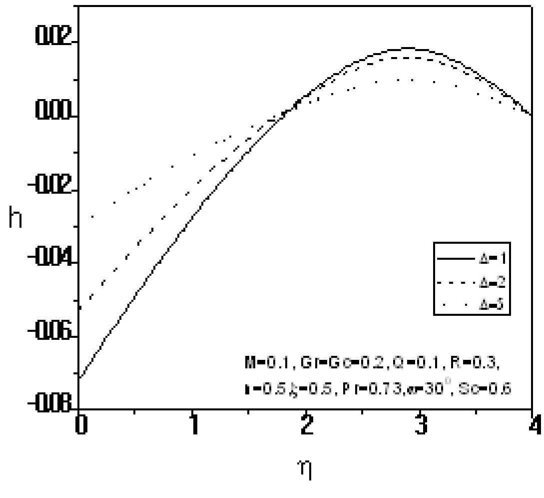

Fig.9 Angular velocity profiles for different Δ

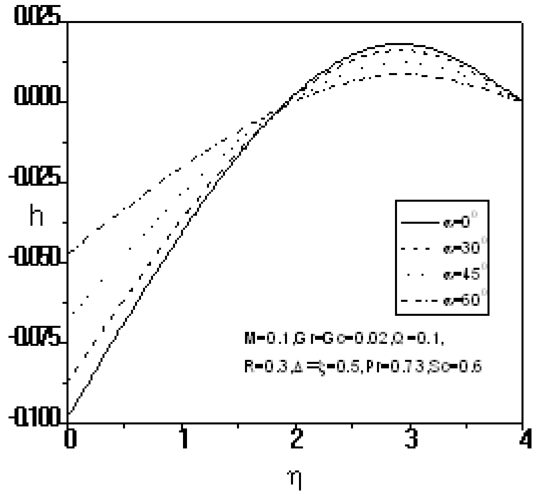

Fig.10 Angular velocity profiles for different α

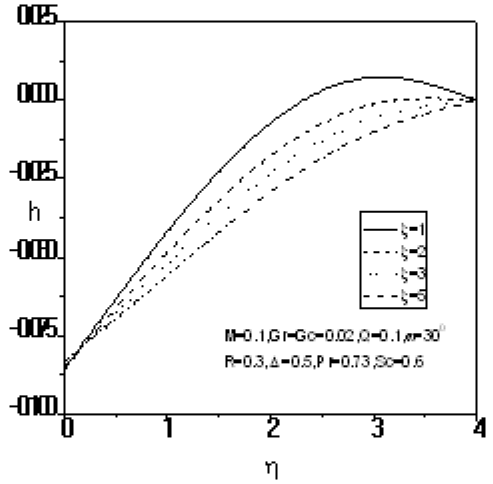

Fig.11 Angular velocity profiles for different ξ values

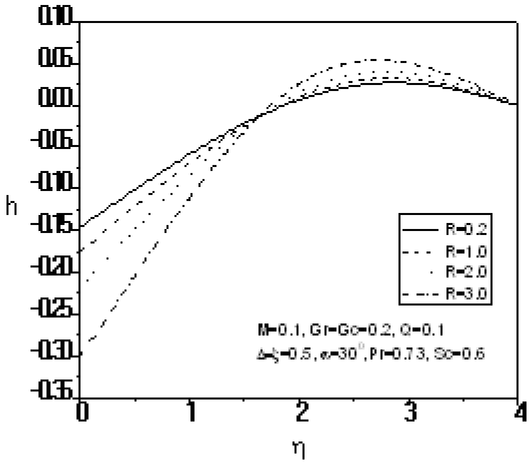

Fig.12 Angular velocity profiles for different *R*

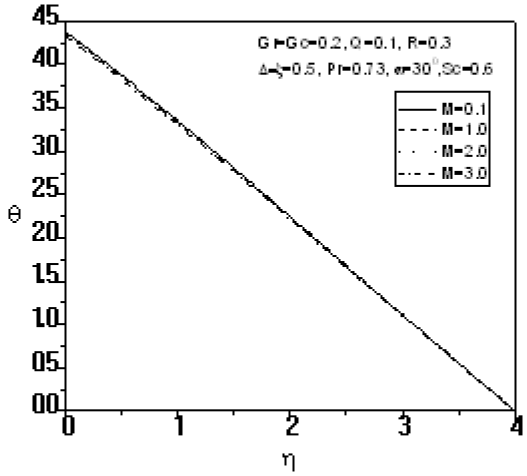

Fig.13 Temperature profiles for different *M*

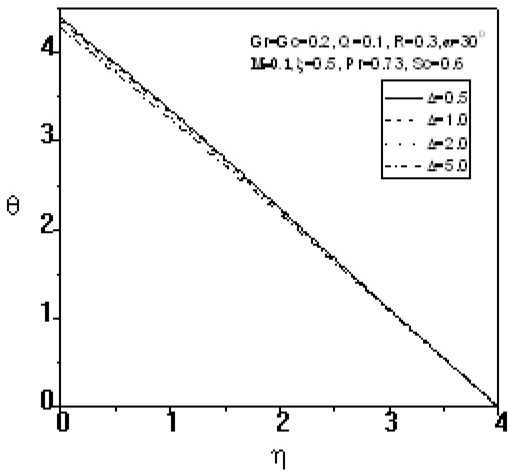

Fig.14 Temperature profiles for different Δ

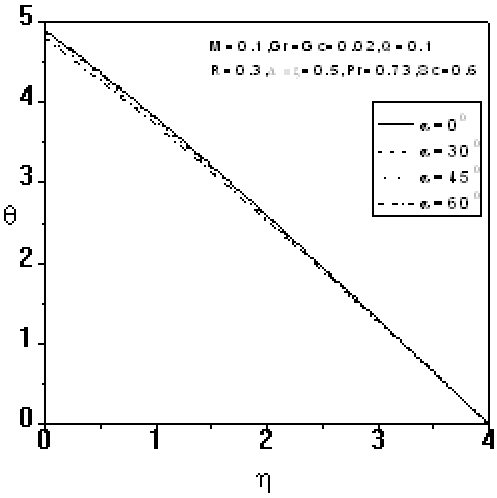

Fig.15 Temperature profiles for different α

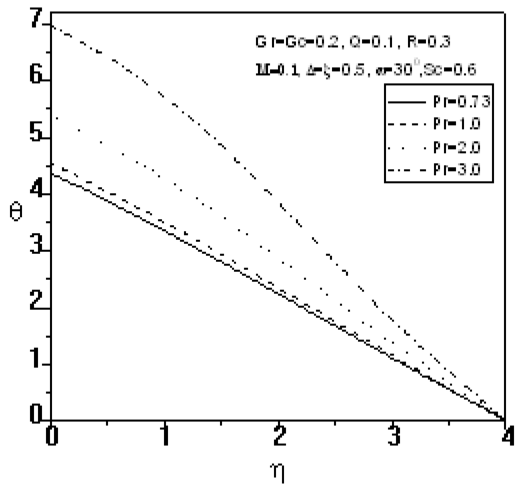

Fig.16 Temperature profiles for different *Pr*

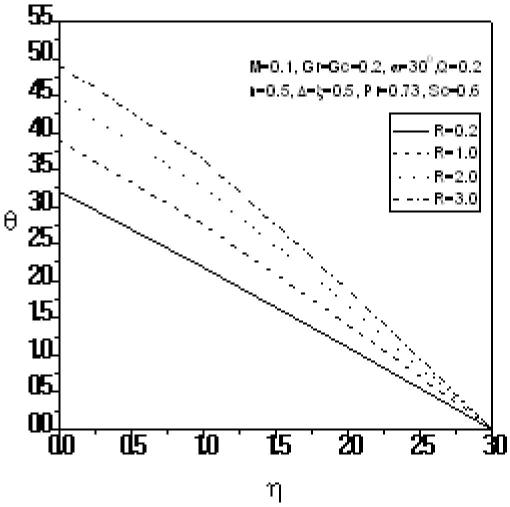

Fig.17 Temperature profiles for different *R*

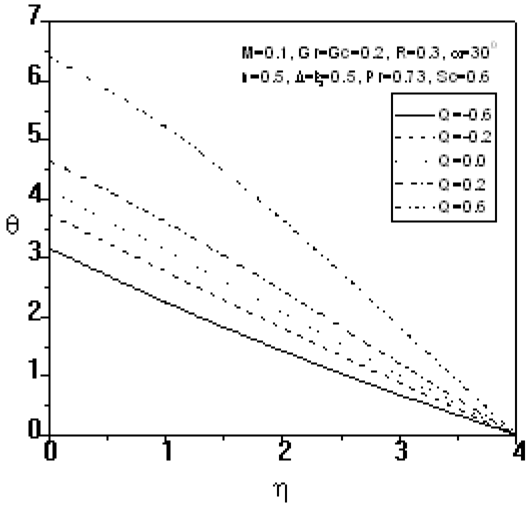

Fig.18 Temperature profiles for different *Q*

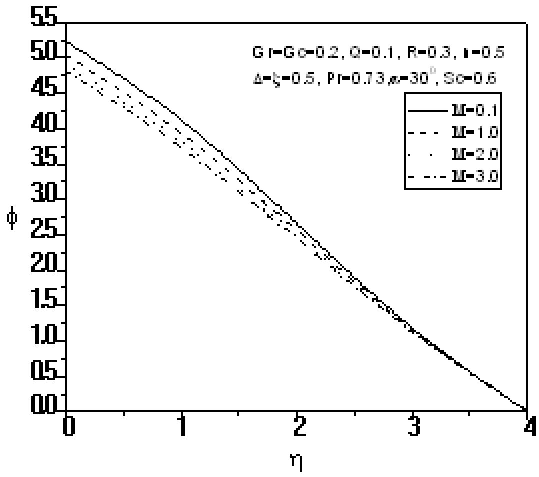

Fig.19 Concentration profiles for different *M*

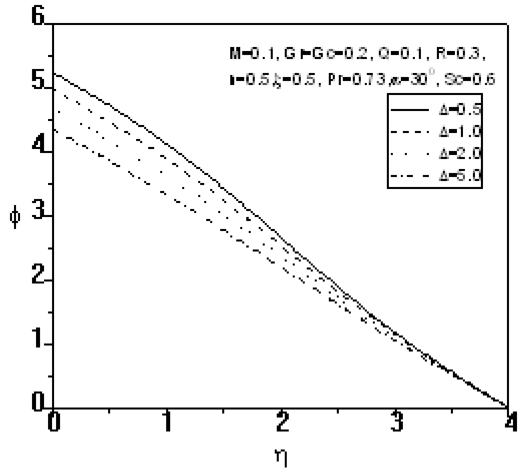

Fig.20 Concentration profiles for different Δ

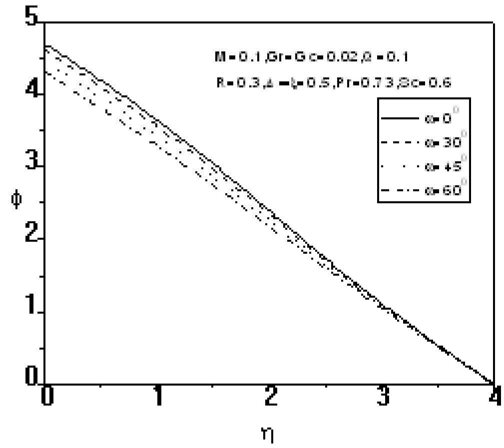

Fig.21 Concentration profiles for different α

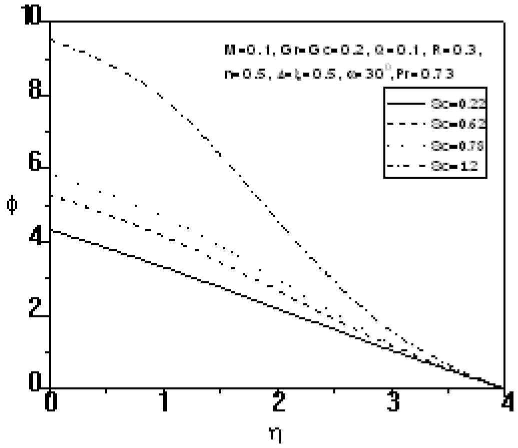

Fig.22 Concentration profiles for different

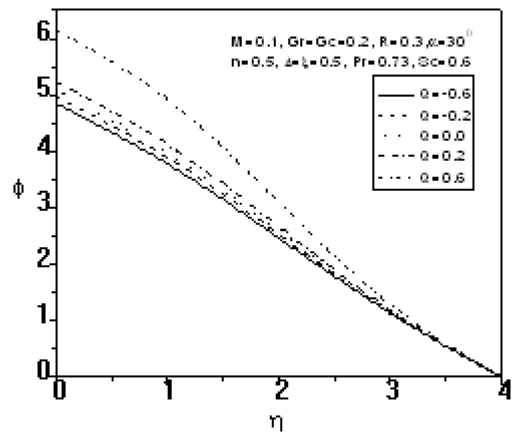

Fig.23 Concentration profiles for different *Q*

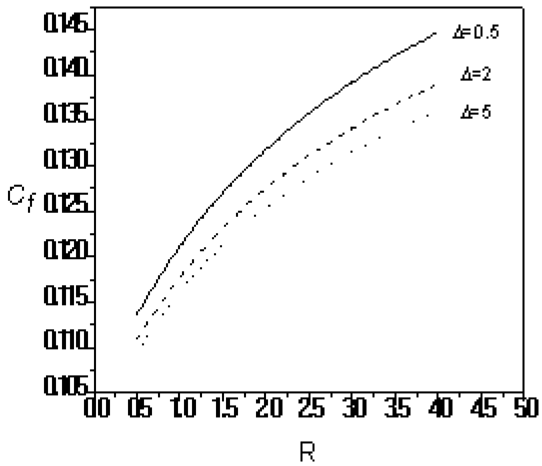

Fig.24 local skin-friction for different Δ

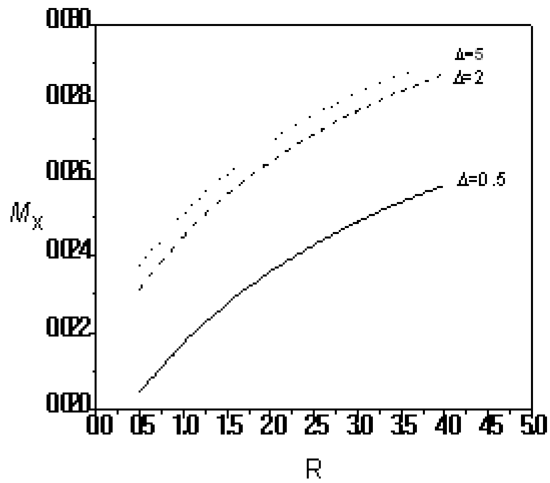

Fig.25 Rate of coupling for different Δ

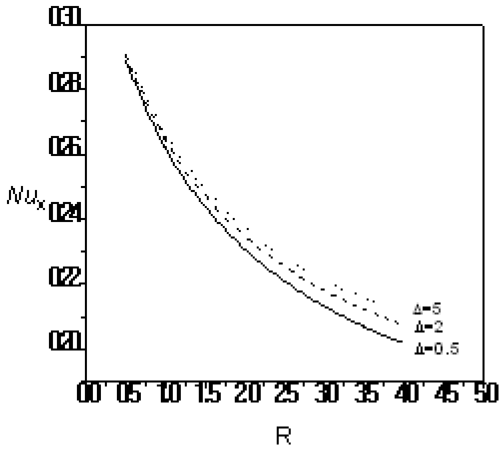

Fig.26 Nusselt number for different Δ

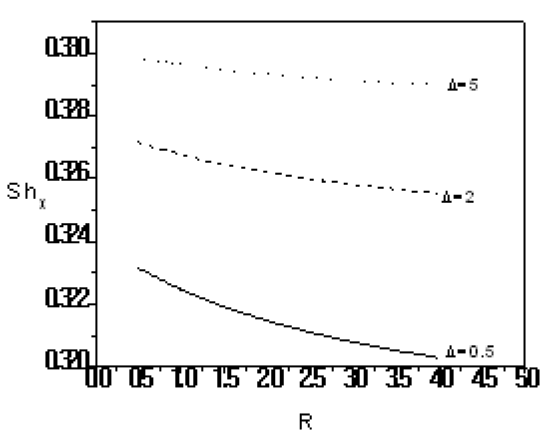

Fig.27 Sherwood number for different values of Δ

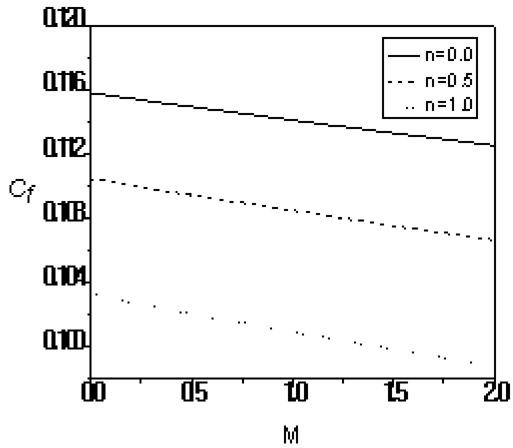

Fig.28 local skin-friction for different *n*

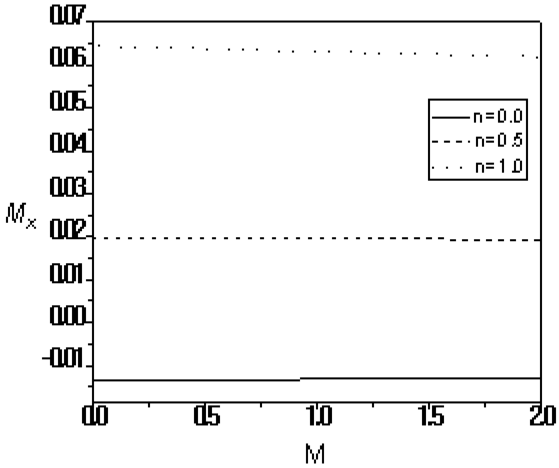

Fig.29 Rate of coupling for different *n*

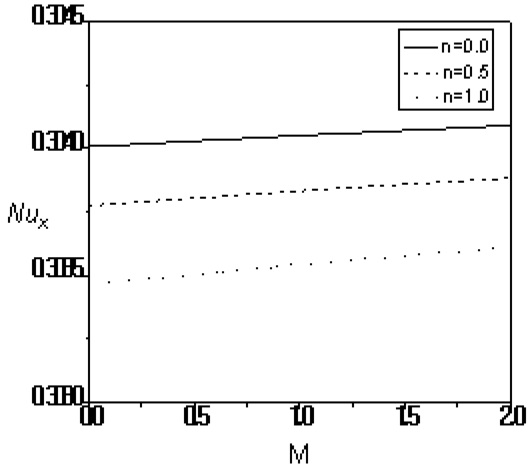

Fig.30 Nusselt number for different *n*

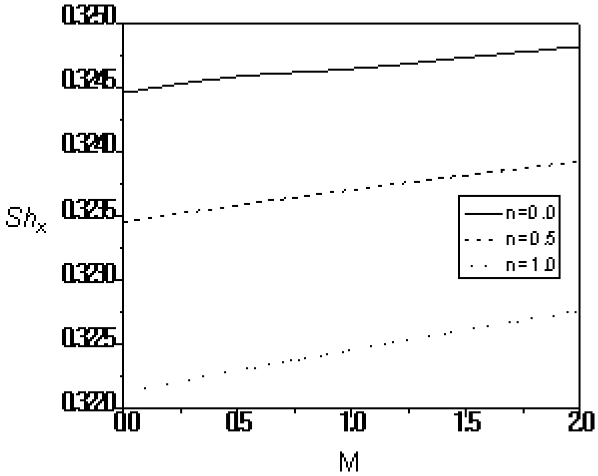

Fig.31 Sherwood number for different values of *n*

References

[1] Ariman T, Turk MA and Sylvester ND . Micro-continuum fluid mechanics - a review. *International Journal of Engineering Sciences*, **1974**,Vol.12, pp.273-293.
[2] Hoyt JW and Fabula AG. *The effect of additives on fluid friction*, **1964**,U.S. Naval Ordnance Test Station Report.
[3] Eringen AC. Theory of micropolar fluids. *Journal of Mathematics and Mechanics*, **1966**,Vol.16**,** pp.1-18.
[4] Gebhart B and Pera L. The nature of vertical natural convection flows resulting from the combined buoyancy effects of thermal and mass diffusion. *International Journal of Heat and Mass Transfer*, **1971,** Vol.14, pp.2025-2050.
[5] Rawat S and Bhargava R. Finite element study of natural convection heat and mass transfer in a micropolar fluid saturated porous regime with Soret/Dufour effects. *International Journal of Applied Mathematics and Mechanics* , **2009**, Vol.5, pp. 58–71.
[6] Joneidi AA, Ganji DD, and Babaelahi M .Micropolar flow in a porous channel with high mass transfer. *International Communications in Heat and Mass Transfer*, **2009**, Vol.36, pp.1082–1088.
[7] Watanabe T and Pop I .Thermal boundary layers in magneto hydrodynamic flow over a flat plate in the presence of transverse magnetic field. *Acta Mechanica*, **1994**, Vol.105, pp.233-238.
[8] Rahman MM and Sattar M A .Magnetohydrodynamic convective flow of a micropolar fluid past a continuously moving vertical porous plate in the presence of heat generation/absorption. *ASME Journal of Heat Transfer*, **2006**, Vol.128, pp.142-152.
[9] Alam MS, Rahman MM and Samad MA. Numerical study of the combined free-forced convection and mass transfer flow past a vertical porous plate in a porous medium with heat generation and thermal diffusion.*Nonlinear Analysis and Modeling Control*, **2006,**Vol.11, pp.331–343.
[10] Alam MS, Rahman MM and Samad MA .Effects of thermophoresis and chemical reaction on unsteady hydro magnetic free convection and mass transfer flow past an impulsively started infinite inclined porous plate in the presence of heat generation/absorption. *International Journal of Science and Technology*,**2007**, Vol.12, pp.44-52.
[11] Alam MS, Rahman MM and Samad MA .Effects of variable suction and thermophoresis on steady MHD combined free-forced convective heat and mass transfer flow a semi-infinite permeable inclined plat in the presence of thermal radiation. *International Journal of Thermal Sciences*, **2008**(in press, available online).
[12] Molla MM, Hossain MA and Yao LS .Natural convection flow along a vertical wavy surface with uniform surface temperature in presence of heat generation/absorption. *International Journal of Thermal Sciences* , **2004**, Vol.43, pp.157–163.

[13] Vajravelu K and Hadjinicolaou A .Heat transfer in viscous fluid over a stretching sheet with viscous dissipation and internal heat generation. *International Communication of Heat and Mass Transfer*, **1993**, Vol.20, pp.417–430.
[14] Mohammadein AA and Gorla RSR .Heat transfer in a micropolar fluid over a stretching sheet with viscous dissipation and internal heat generation. *International Journal of Numerical Methods of Heat and Fluid Flow*, **2001**, Vol.11, pp. 50-58.
[15] Ishak A .Thermal boundary layer flow over a stretching sheet in a micropolar fluid with radiation effect. *Meccanica*, **2010**, Vol.45, pp.367-373.
[16] Muhammad Ashraf and Muhammad .MHD boundary layer stagnation point flow and heat transfer of a micropolar Fluid towards a Heated Shrinking Sheet with Radiation and Heat Generation. *Rashid World Applied Sciences Journal*, **2012**, Vol.16, No.10, pp.1338-1351.
[17] Ahmed Yousof Bakier .Natural convection heat and mass transfer in a micropolar fluid- saturated non-Darcy porous regime with radiation and thermophoresis effects. *Thermal science*, **2011**, Vol. 15, suppl. 2, pp. s317-s326.
[18] Rahman MM and Sattar MA .Transient convective flow of micropolar fluid past a continuously moving vertical porous plate in the presence of radiation. *International Journal of Applied and Mathematical Engineering*, **2007**, Vol.12, pp.497-513.
[19] Mansour MA, Al-Hakiem MA and El-Kabeir SM .Heat and mass transfer in magnetohydrodynamic flow of micropolar fluid on a circular cylinder with uniform heat and mass flux. *Journal of Magnetism and Magnetic Materials*, **2000**, Vol. 220, pp.259–270.
[20] Damseh A, Al-Azab A, Shannak A and Al-Husein M .Unsteady natural convection heat transfer of micropolar fluid over a vertical surface with constant heat flux. *Turkish journal of Engineering and Environmental Sciences*, **2007**, Vol.31, pp. 225 – 233.
[21] Srinivasacharya D and Ramreddy Ch .Effects of soret and dufour on mixed convection heat and mass transfer in a micropolar fluid with heat and mass fluxes. *International Journal of Applied Mathematics and Mechanics*, **2010**, Vol.6, No.21, pp.8-21.
[22] Jashim Uddin Md. Convective flow of micropolar fluids along an inclined flat plate with variable electric conductivity and uniform surface heat flux. *Daffodil International university journal of science and technology*, **2011**, Vol.6, issue 1, pp. 69-79.
[23] Rahman MM and Sultana T . Convective flow of a micropolar fluid past a vertical porous plate immersed in a porous medium in the presence of radiation. *Journal of Computation and Applied Mechanics*, **2008** (accepted).
[24] Markin JH and Mahmood T .Similarity solution for Mixed convection boundary layer prescribed heat flux. *Zeitschrift fuer Angewandte Mathematik und Physik*, **1989**, Vol.40, pp. 61–68.
[25] Brewster M.Q., *Thermal radiative transfer and properties*, John Wiley & Sons, **1992**, New York.
[26] Jain MK, Iyengar SRK and Jain RK *Numerical Methods for Scientific and Engineering Computation*, **1985**, Wiley Eastern Ltd., New Delhi, India.